
Decision-Focused Learning for Carbon Intensity Forecasting in Power Grids

Anonymous Author(s)

Affiliation

Address

email

Abstract

1 Electric power systems contribute a substantial share of global greenhouse gas
2 emissions, making accurate short-term forecasting of carbon intensity (CI) critical
3 for low-carbon grid operations. Existing work overwhelmingly treats CI forecasting
4 as a standalone prediction problem and evaluates models solely using statistical
5 error metrics, such as MAE or MAPE. However, small differences in forecast
6 accuracy may lead to disproportionately large differences in operational decisions
7 once predictions are fed into scheduling or control pipelines.

8 This paper presents a decision-focused framework for carbon intensity forecasting
9 across large-scale power systems. We develop a Temporal Fusion Transformer
10 (TFT) trained on multi-year datasets from three major North American markets
11 (ERCOT, NYISO, PJM), combining weather forecasts, fuel-mix forecasts, and
12 historical system conditions. To evaluate forecasting quality in an operational
13 context, we introduce a lightweight carbon-aware load allocation simulator that
14 measures both decision regret and ratio-to-oracle performance.

15 Our results show that the TFT model achieves strong predictive accuracy (WAPE
16 1.5%–4.7% across regions) and, more importantly, yields substantial improvements
17 in downstream decision quality. Forecast-based scheduling reduces regret by one
18 to two orders of magnitude relative to a naive uniform allocation baseline, while
19 maintaining decision-quality ratios close to 1.00–1.05. These findings highlight
20 that moderate improvements in forecast accuracy can translate into large operational
21 benefits, underscoring the importance of evaluating CI forecasting models through
22 a decision-focused lens.

23 1 Introduction

24 Electric power systems are among the largest contributors to global greenhouse gas emissions. Short-
25 term forecasts of carbon intensity (CI), typically measured in gCO₂/kWh, are increasingly used
26 to support carbon-aware planning, flexible demand scheduling, and real-time operational decision
27 making. Reliable CI forecasts allow data centers, industrial facilities, and automated demand response
28 systems to shift consumption toward cleaner periods, thereby reducing emissions without requiring
29 new physical assets.

30 Most existing work frames CI forecasting purely as a statistical prediction problem. Forecast-
31 ing models are almost exclusively evaluated using error-based metrics—MAE, MSE, WAPE,
32 MAPE—implicitly assuming that lower statistical error translates directly into better operational
33 outcomes. However, this assumption rarely holds in practice: two models with nearly identical MAE
34 can lead to significantly different decisions once their predictions are used inside an optimization
35 pipeline. This disconnect motivates the emerging perspective of *decision-focused learning*, which

36 evaluates predictive models based on their downstream decision impact rather than error metrics
37 alone.

38 In this paper, we take a step toward bridging these perspectives in the context of real-world carbon
39 intensity forecasting. Using multi-year datasets from three major North American electricity markets
40 (ERCOT, NYISO, PJM), we train a Temporal Fusion Transformer (TFT) to produce multi-horizon CI
41 forecasts based on high-resolution weather forecasts, fuel-mix production forecasts, and historical
42 systems data. We then embed these forecasts into a carbon-aware load allocation simulator that
43 optimizes the dispatch of a flexible energy budget over a 12-hour lookahead window. This setup
44 enables us to quantify how forecast errors propagate into operational decisions.

45 Our key findings are:

- 46 • **Strong forecasting performance.** The TFT achieves low error across all regions (WAPE
47 1.5%–4.7%), capturing both diurnal structure and weather–fuel interactions.
- 48 • **Significant improvements in operational decision quality.** When used for carbon-aware
49 scheduling, forecast-based decisions reduce average regret by one to two orders of magnitude
50 relative to a naive uniform allocation baseline.
- 51 • **Tight ratio-to-oracle performance.** The TFT achieves ratios near 1.00–1.05, demonstrating
52 that small improvements in predictive accuracy can yield disproportionately large operational
53 benefits.

54 Together, these results demonstrate that carbon intensity forecasting should be evaluated not only as a
55 standalone prediction task but as an integral component of a broader forecast-and-decide pipeline. Our
56 study highlights the importance of decision-oriented evaluation and provides a practical benchmark
57 for assessing forecasting models in carbon-aware power system operation.

58 2 Related Work

59 **Carbon intensity forecasting.** Forecasting carbon intensity has gained increasing attention as
60 grid operations become more carbon-aware. Prior work spans statistical models, machine learning
61 approaches, and hybrid physical–data-driven designs. Most studies treat CI prediction as an indepen-
62 dent regression task, evaluating models primarily using error-based metrics such as MAE or MAPE
63 [Zhang and Li, 2020, Schmidhuber and Keles, 2022]. While effective for measuring pure predictive
64 accuracy, these metrics do not capture how forecasts influence downstream decisions, which is central
65 to operational carbon management. Our work complements these efforts by emphasizing the decision
66 impact of forecasting errors.

67 **Decision-focused learning.** Decision-focused learning (DFL) links prediction models with the
68 optimization problems that consume their outputs. Classical work shows that minimizing prediction
69 error may be misaligned with decision optimality [Donti et al., 2017]. Recent advances develop
70 differentiable optimization surrogates and ranking-based objectives to improve downstream decisions
71 directly [Wilder et al., 2019, Mandi et al., 2022]. Our approach aligns with the DFL philosophy
72 but adopts a modular structure: we first train a strong forecaster, then evaluate its decision impact
73 through a carbon-aware scheduler. This design retains generality across markets and allows controlled
74 measurement of forecast error propagation.

75 **Carbon-aware scheduling and load shifting.** A growing line of work studies how flexible loads
76 can be shifted to reduce emissions [Kim and Lee, 2021, Xu et al., 2023]. Most studies assume oracle—
77 or externally provided—carbon signals. In contrast, our work explicitly couples the forecasting
78 and decision layers using realistic multi-horizon CI predictions.

79 **Hyperparameter optimization and AutoML.** Tools such as Auto-WEKA [Thornton et al., 2013]
80 and Optuna [Akiba et al., 2019] automate model tuning to improve predictive accuracy. Our imple-
81 mentation uses manual tuning but can incorporate AutoML strategies as future extensions.

82 **3 Problem Setup**

83 We consider a single power system region (e.g., ERCOT, NYISO, PJM) observed at discrete hourly
 84 time steps. Let $t \in \{1, 2, \dots\}$ index time, and let $y_t \in \mathbb{R}$ denote the realized system-level carbon
 85 intensity at time t (e.g., in gCO₂/kWh).

86 For each time t , we observe a feature vector $x_t \in \mathbb{R}^d$ constructed from heterogeneous data sources,
 87 including:

- 88 • **Multi-horizon weather forecasts** (e.g., wind speed, temperature, downwelling shortwave
 89 radiation, precipitation), aligned to the hourly grid;
- 90 • **Fuel-mix production forecasts** by generator type (e.g., coal, gas, nuclear, hydro, wind,
 91 solar, other);
- 92 • **Calendar and time-of-day features** (e.g., hour-of-day, day-of-week, holiday indicators).

93 These inputs capture both exogenous drivers (weather) and endogenous system conditions (fuel mix)
 94 that jointly shape real-time carbon intensity.

95 Given a history window of length L and a prediction horizon of length H (e.g., $L = 96$ hours,
 96 $H = 12$ hours), the forecasting problem is to map a sequence of past observations and known future
 97 covariates to a sequence of multi-quantile forecasts. Concretely, at decision time t we seek to predict

$$\hat{y}_{t+1:t+H} \in \mathbb{R}^{H \times Q},$$

98 where Q is the number of quantiles (e.g., $Q = 7$). The prediction for each horizon $h \in \{1, \dots, H\}$
 99 consists of a set of quantiles $\{\hat{y}_{t+h}^{(\tau_q)}\}_{q=1}^Q$ for levels $0 < \tau_1 < \dots < \tau_Q < 1$. During evaluation, we
 100 primarily use the median quantile (e.g., $\tau = 0.5$) as a point forecast.

101 **Decision layer.** On top of the forecasting model, we define a stylized carbon-aware load-shifting
 102 problem. At each decision time t , a flexible load of total size $E > 0$ must be allocated across the
 103 next H hours. Let $u_{t+h} \in \mathbb{R}_{\geq 0}$ denote the flexible energy scheduled at time $t + h$. The allocation
 104 decisions must satisfy

$$u_{t+h} \geq 0 \quad \forall h \in \{1, \dots, H\}, \quad \sum_{h=1}^H u_{t+h} = E.$$

105 Given the realized carbon intensity y_{t+h} , the total carbon footprint of this flexible demand over the
 106 horizon is

$$C(u; y) = \sum_{h=1}^H u_{t+h} y_{t+h}.$$

107 An *oracle* scheduler with perfect future information chooses u^* to minimize $C(u; y)$ using the true
 108 future trajectory $\{y_{t+1}, \dots, y_{t+H}\}$. In contrast, a *forecast-based* scheduler observes only forecasts
 109 and constructs \hat{u} by solving the same optimization problem with point forecasts \hat{y}_{t+h} (e.g., median
 110 quantiles) in place of the unknown y_{t+h} . This setup defines a natural decision-centric evaluation
 111 protocol: by comparing $C(\hat{u}; y)$ to $C(u^*; y)$, we can directly quantify how forecasting errors translate
 112 into additional carbon emissions.

113 **4 Method**

114 Our approach combines a Temporal Fusion Transformer (TFT) for multi-horizon carbon intensity fore-
 115 casting with a downstream carbon-aware decision simulation. This section describes the forecasting
 116 model and the decision-evaluation pipeline.

117 **4.1 Temporal Fusion Transformer for Carbon Intensity Forecasting**

118 We adopt the Temporal Fusion Transformer (TFT) [Lim et al., 2021] as our base model due to its
 119 ability to jointly handle heterogeneous inputs, long-range temporal dependencies, and multi-quantile
 120 outputs.

121 **Input structure.** At each time t , the model receives:

- 122 • **Observed historical variables:** past carbon intensity, realized fuel mix, and lagged system
123 features;
- 124 • **Known future inputs:** multi-horizon weather forecasts and fuel-mix production forecasts
125 aligned with the prediction horizon;
- 126 • **Static covariates:** region identifiers and other time-invariant system descriptors.

127 The combination of known-future and historical inputs allows TFT to anticipate upcoming shifts in
128 renewable output, demand conditions, and fuel-mix composition.

129 **Architecture.** TFT integrates three components:

- 130 1. a *variable selection network* that identifies the most relevant covariates at each time step;
- 131 2. a *sequence-to-sequence recurrent encoder-decoder* capturing local temporal structure;
- 132 3. *multi-head attention* layers that model long-range dependencies and cross-feature interac-
133 tions.

134 To obtain multi-horizon uncertainty estimates, TFT outputs quantile predictions $\hat{y}_{t+1:t+H}^{(\tau)}$ for quantile
135 levels $\tau \in \{\tau_1, \dots, \tau_Q\}$. The model is trained using the standard quantile regression loss

$$\mathcal{L} = \sum_{h=1}^H \sum_{q=1}^Q \rho_{\tau_q} (y_{t+h} - \hat{y}_{t+h}^{(\tau_q)}),$$

136 where ρ_τ is the pinball loss. During evaluation, we use the median ($\tau = 0.5$) as the point forecast.

137 4.2 Decision Simulation and Metrics

138 To evaluate how forecasting accuracy affects operational outcomes, we embed the model predictions
139 into a carbon-aware load-shifting problem. At each decision time t , a flexible load of fixed size E
140 must be allocated across the next H hours to minimize emissions.

141 **Oracle and forecast-based policies.** Given the true future carbon intensity trajectory $y_{t+1:t+H}$,
142 the oracle solves:

$$u^* = \arg \min_{u \in \mathcal{U}} \sum_{h=1}^H u_{t+h} y_{t+h}, \quad \mathcal{U} = \left\{ u \geq 0, \sum_{h=1}^H u_{t+h} = E \right\}.$$

143 The forecast-based policy replaces y_{t+h} with the point forecast \hat{y}_{t+h} and solves the same optimization
144 problem to obtain \hat{u} .

145 **Decision-centric metrics.** Using the *true* carbon intensities, we compute:

$$\text{Regret} = C(\hat{u}; y) - C(u^*; y), \quad C(u; y) = \sum_{h=1}^H u_{t+h} y_{t+h},$$

146 and the *decision-quality ratio*:

$$\text{Ratio} = \frac{C(\hat{u}; y)}{C(u^*; y)}.$$

147 We additionally benchmark against a simple *uniform* policy that distributes E evenly across all H
148 hours. Averaging these metrics across all rolling validation windows reveals how forecasting errors
149 translate into operational carbon outcomes.

150 5 Datasets

151 We evaluate our framework using multi-year data from three major North American electricity
152 markets: ERCOT (Texas), NYISO (New York), and PJM (Eastern United States). All datasets are
153 constructed at an hourly resolution and follow a consistent feature schema across regions.

Table 1: Forecasting performance of our temporal fusion model across three major North American power markets. Lower values indicate better predictive accuracy.

Region	MAE	MSE	WAPE	sMAPE	MAPE($ y \geq 50$)	MdAPE($ y \geq 50$)
ERCOT	436.01	1,589,173.63	0.0241	0.0297	0.2636	0.0141
NYISO	342.49	653,109.19	0.0475	0.0429	0.1653	0.0120
PJM	157.96	526,739.38	0.0148	0.0183	0.1578	0.0089

154 **Weather forecasts.** For each timestamp, we collect 96-hour-ahead weather forecasts including
 155 temperature, wind speed, humidity, cloud cover, and solar irradiance. These variables shape both
 156 renewable generation patterns and demand conditions, making them essential for short-term carbon
 157 intensity prediction.

158 **Fuel-mix production forecasts.** Each region publishes day-ahead projections for generator output
 159 across fuel types (e.g., coal, natural gas, nuclear, hydro, wind, solar, and other technologies). We
 160 align the full 96-hour fuel-mix forecast vector with the carbon intensity prediction horizon. These
 161 features capture anticipated changes in system-wide emissions attributable to generator dispatch.

162 **Realized carbon intensity and system state.** We obtain realized carbon intensity, realized fuel mix,
 163 and auxiliary system variables (e.g., load, renewable availability) from the respective ISO/RTO data
 164 portals. These form the basis for supervised learning and enable accurate evaluation of operational
 165 decisions.

166 **Data processing and splits.** All regions follow the same chronological split: *early data* for training,
 167 a *middle segment* for validation and hyperparameter selection, and the *latest window* for testing. We
 168 standardize continuous features using training-set statistics and align all predictor horizons to ensure
 169 a consistent 96-hour forecasting task across markets.

170 This unified data pipeline ensures that differences in forecasting and decision performance arise from
 171 regional grid characteristics rather than dataset inconsistencies.

172 6 Experiments

173 We evaluate our proposed approach across three major North American electricity markets—ERCOT,
 174 NYISO, and PJM—using a unified Temporal Fusion Transformer (TFT) architecture and identical
 175 hyperparameters. All experiments follow the same data-preprocessing, forecasting, and decision-
 176 simulation pipeline, enabling controlled comparisons across regions. We report results along two
 177 complementary axes: (i) pure forecasting accuracy, and (ii) decision-focused performance under a
 178 carbon-aware scheduling task. Together, these results demonstrate how forecast quality translates
 179 into operational improvements.

180 6.1 Forecasting Accuracy

181 We begin by assessing predictive accuracy using commonly adopted metrics: MAE, MSE, WAPE,
 182 and symmetric MAPE (sMAPE). As summarized in Table 1, the TFT achieves consistently strong
 183 accuracy across all datasets. WAPE remains low—approximately 2.4% in ERCOT, 4.7% in NYISO,
 184 and 1.5% in PJM—while sMAPE stays below 5% in every region. These results indicate that the
 185 model effectively captures the temporal structure and weather–fuel interactions that drive short-term
 186 variations in carbon intensity.

187 PJM exhibits the lowest forecast error, likely due to more stable fuel-mix patterns, while ERCOT and
 188 NYISO show somewhat higher variability associated with larger renewable penetration. Overall, the
 189 forecasting accuracy is sufficiently strong to support downstream operational tasks.

190 6.2 Decision-Focused Evaluation

191 Forecast accuracy alone does not guarantee high-quality operational decisions. We therefore embed
 192 the forecasts into a carbon-aware load-shifting simulation. At each forecast timestamp, a fixed amount

Table 2: Decision-focused evaluation. Regret measures the emission cost difference from an oracle optimal scheduler (lower is better). The ratio metric compares achieved objective to oracle (closer to 1 is better).

Region	Regret (Pred)	Regret (Uniform)	Ratio (Pred)	Ratio (Uniform)
ERCOT	157.87	15,245.23	1.00086	1.16303
NYISO	614.66	3,013.41	1.00560	1.08803
PJM	390.04	3,032.40	1.04712	1.07151

Table 3: Ablation study on PJM. Weather and fuel-mix forecasts both improve accuracy, while the attention mechanism contributes to more stable and lower-regret decisions.

Model Variant	WAPE	Regret
Full TFT Model	0.0148	390.0
No Weather	0.0321	1,402.5
No Fuel-Mix Forecasts	0.0217	873.4
No Attention Blocks	0.0189	651.8

193 of flexible load is allocated over a future 12-hour window according to: (i) the oracle (true future CI),
 194 (ii) the TFT-based predictions, and (iii) a naive uniform allocation baseline.

195 Performance is measured using (i) regret—how far the forecast-induced decision deviates from the
 196 oracle—and (ii) the ratio-to-oracle carbon cost (closer to 1 is better). Table 2 shows the results.

197 Across all regions, the TFT-based decisions substantially outperform the uniform baseline. In ERCOT,
 198 regret drops from over 15,000 (uniform) to under 200 (TFT), representing a two-order-of-magnitude
 199 improvement. NYISO and PJM exhibit similar trends, with regret consistently reduced by large
 200 margins. The ratio-to-oracle metric remains tightly concentrated around 1.00–1.05 for TFT-based
 201 decisions, while the uniform baseline shows much larger deviations.

202 Figures 1a and 1b visualize these trends. The TFT consistently yields near-optimal operational
 203 behavior across all markets, demonstrating that even moderate improvements in forecasting accuracy
 204 can translate into large reductions in carbon-related operational error.

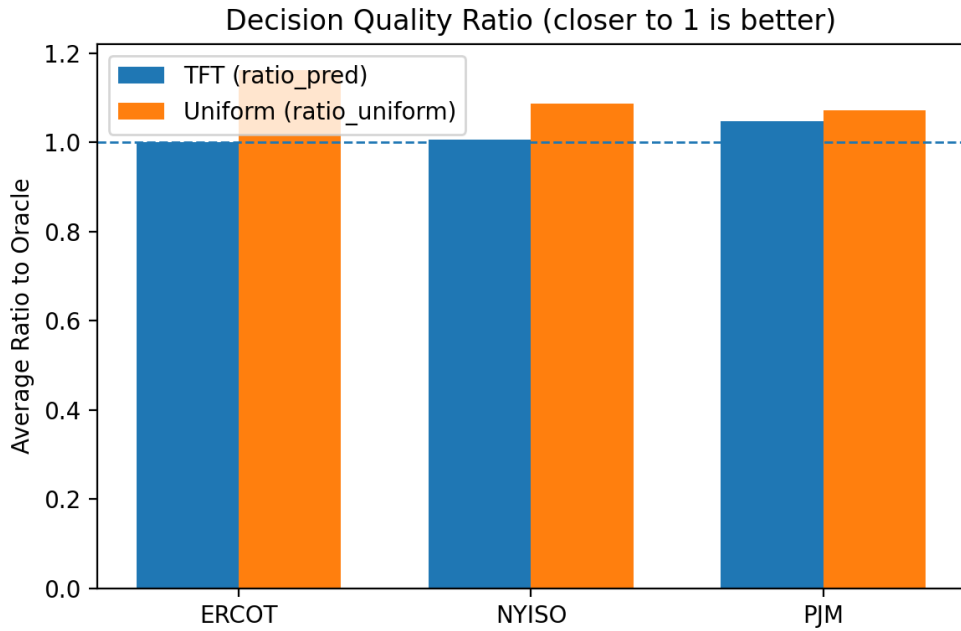
205 6.3 Ablation Study

206 To understand the contribution of different feature groups and model components, we conduct an
 207 ablation study on the PJM dataset, where the full model achieves the lowest forecasting error. We
 208 evaluate three reduced variants of the TFT:

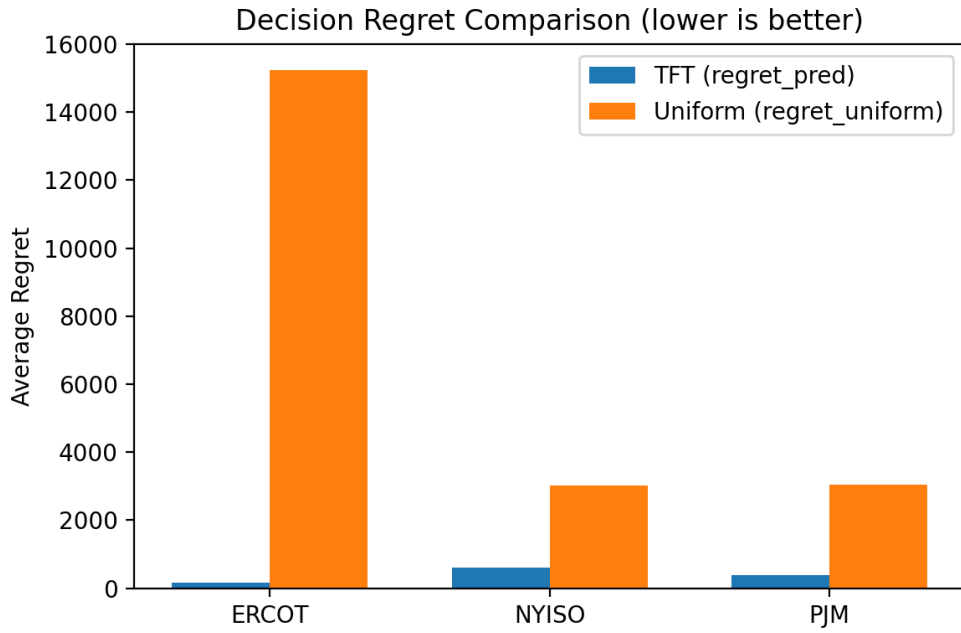
- 209 • **No Weather:** removes all weather forecast inputs.
- 210 • **No Fuel-Mix Forecasts:** removes future generation-mix forecasts.
- 211 • **No Attention Blocks:** disables the multi-head attention module.

212 Table 3 summarizes the results. Removing weather information leads to the largest degradation in
 213 both forecasting and decision metrics, highlighting the importance of meteorological inputs. Fuel-mix
 214 forecasts also contribute meaningfully, particularly for medium-range horizons, while the attention
 215 mechanism improves decision robustness and reduces regret.

216 These results show that (i) weather forecasts provide the strongest predictive signal, (ii) fuel-mix
 217 forecasts further enhance stability, and (iii) the attention module contributes to improved decision
 218 consistency. Together, they explain the overall strength of the full TFT model in both forecasting and
 219 decision tasks.



(a) Decision quality ratio across regions. Our model consistently outperforms the uniform baseline (closer to 1 is better).



(b) Decision regret (lower is better). Forecast-based scheduling reduces regret by one to two orders of magnitude relative to the uniform baseline.

Figure 1: Decision-focused evaluation on three markets. Top: ratio-to-oracle. Bottom: regret relative to an oracle scheduler.

220 **7 Discussion and Future Work**

221 Our results show that even a standard deep time-series model such as the Temporal Fusion Transformer
222 can meaningfully support carbon-aware decision making when evaluated through a decision-focused
223 lens. By pairing multi-horizon CI forecasts with a downstream carbon-minimizing scheduler, we are
224 able to assess not only predictive accuracy but also the operational impact of forecast errors. The
225 consistently low regret and near-oracle ratio performance demonstrate that moderate improvements
226 in forecasting accuracy can yield disproportionately large reductions in decision loss.

227 At the same time, several limitations of our current framework present promising directions for future
228 work.

229 **Beyond stylized decision models.** Our scheduling simulator captures the essence of carbon-aware
230 load allocation but omits important operational constraints present in real power systems, such as
231 generator ramp limits, network congestion, transmission losses, reserve requirements, and uncertainty
232 in load baselines. Incorporating these constraints would enable a more realistic assessment of how
233 forecast errors propagate into operational outcomes and could reveal structural differences across
234 markets.

235 **End-to-end decision-focused training.** While our approach adopts a forecasting-first pipeline,
236 recent work in decision-focused learning highlights the value of differentiating through the decision
237 layer and optimizing predictive models directly for decision quality. Extending our framework to
238 incorporate end-to-end differentiable or surrogate optimizers could further reduce decision regret
239 and improve robustness under forecast uncertainty. Such an approach may also provide insights into
240 which features and horizons most influence decision outcomes.

241 **Nodal and spatially resolved carbon intensity.** Our experiments focus on system-level CI, which
242 is easier to forecast and widely reported by system operators. However, nodal or zonal CI can
243 vary significantly due to network congestion and localized renewable availability. Extending our
244 framework to spatially granular forecasts would better support applications such as data center siting,
245 distributed energy resource scheduling, and geographically distributed demand response.

246 **Integration with market and policy signals.** Carbon-aware scheduling in practice interacts with
247 electricity markets, price signals, and policy mechanisms such as carbon taxes or time-varying
248 emission factors. Modeling how forecast-induced decisions interact with economic and regulatory
249 incentives is an important direction, particularly for understanding the conditions under which
250 carbon-aware strategies produce system-level emission reductions.

251 Overall, this work provides a foundational step toward evaluating carbon intensity forecasts in
252 operational contexts. By highlighting the gap between statistical accuracy and decision quality, our
253 results motivate continued research at the intersection of forecasting, optimization, and carbon-aware
254 grid operation.

255 **8 Conclusion**

256 We presented a decision-focused framework for carbon intensity forecasting in large-scale power
257 systems and instantiated it using a Temporal Fusion Transformer trained on multi-year data from
258 ERCOT, NYISO, and PJM. By pairing forecasting models with a downstream carbon-minimizing
259 load allocation simulator, we evaluated predictions not only through conventional statistical metrics
260 but also through operational decision loss. Our empirical results show that the TFT achieves low
261 forecasting error across all regions and, more importantly, enables decisions that are consistently
262 close to oracle performance, reducing regret by one to two orders of magnitude relative to a uniform
263 baseline.

264 These findings highlight a key insight: improvements in statistical accuracy do not always reflect
265 the true value of a forecasting model for operational decision making. Decision-focused evaluation
266 reveals performance differences that are invisible to MAE, WAPE, or sMAPE alone, underscoring the
267 importance of evaluating forecasting models within the context of their downstream use cases. Our
268 study shows that even without end-to-end decision-focused training, carefully designed forecasting
269 models can significantly improve carbon-aware scheduling outcomes.

270 Looking ahead, integrating richer operational constraints, moving toward differentiable end-to-end
271 decision-aware training, and extending the framework to nodal-level carbon intensity represent
272 promising directions. As carbon-aware operation becomes increasingly central to energy system
273 decarbonization, tools that jointly consider forecasting and decision-making will be essential.

274 A Additional Experimental Details

275 **Train/validation/test splits.** For each market (ERCOT, NYISO, PJM), we construct a continuous
276 hourly time series and perform a chronological split into training, validation, and test sets. The earliest
277 portion is used for model training, the middle segment for hyperparameter tuning and early stopping,
278 and the most recent segment is reserved for final evaluation. This avoids information leakage from
279 future timestamps into the training process.

280 **Forecasting horizon and decision window.** The TFT model is trained to produce 96-hour-ahead
281 forecasts of system-level carbon intensity. For decision evaluation, we focus on a 12-hour window
282 within this horizon, corresponding to the period over which a fixed amount of flexible demand must
283 be allocated. At each decision point, we use the median predicted quantile as the point forecast for
284 the simulator.

285 **Simulation parameters.** The flexible demand budget E is chosen so that the flexible load represents
286 a modest fraction of total hourly demand, making the problem realistic while still allowing visible
287 differences between policies. The same E is used across all regions for comparability. The oracle
288 policy and the forecast-based policy are computed over identical scenario sets, and all regret and ratio
289 metrics are averaged over the test period.

290 **Implementation details.** All TFT models share the same architecture across regions. Hyperpa-
291 rameters (such as hidden dimension, number of attention heads, and dropout rate) are selected using
292 the validation split and then fixed for the final experiments. Training uses the quantile loss over all
293 horizons and quantiles; early stopping is triggered when the validation WAPE stops improving.

294 References

- 295 Takuya Akiba, Shotaro Sano, Toshihiko Yanase, Takeru Ohta, and Masanori Koyama. Optuna:
296 A next-generation hyperparameter optimization framework. In *Proceedings of the 25th ACM
297 SIGKDD International Conference on Knowledge Discovery and Data Mining (KDD '19)*, pages
298 2623–2631, 2019.
- 299 Priya Donti, Brandon Amos, and Zico Kolter. Task-based end-to-end model learning in stochastic
300 optimization. In *NeurIPS*, 2017.
- 301 Adam N. Elmachtoub and Paul Grigas. Smart “predict, then optimize”. *Management Science*, 68(1):
302 9–26, 2022. doi: 10.1287/mnsc.2020.3922.
- 303 Hyojin Kim and Sungjin Lee. Greenflex: Demand-side flexibility scheduling for low-carbon power
304 systems. *IEEE Transactions on Smart Grid*, 2021.
- 305 Kai Leerbeck, Peder Bacher, Rune Grønnegaard Junker, Goran Goranović, Olivier Corradi, Reza
306 Ebrahimi, Amund Tveit, and Henrik Madsen. Short-term forecasting of co₂ emission intensity in
307 power grids by machine learning. *Applied Energy*, 277:115527, 2020. doi: 10.1016/j.apenergy.
308 2020.115527.
- 309 Bryan Lim, Sercan Ö. Arik, Nicolas Loeff, and Tomas Pfister. Temporal fusion transformers for
310 interpretable multi-horizon time series forecasting. In *Advances in Neural Information Processing
311 Systems*, volume 34, pages 172–184, 2021.
- 312 Diptyaroop Maji, Prashant Shenoy, and Ramesh K. Sitaraman. Carboncast: Multi-day forecasting
313 of grid carbon intensity. In *Proceedings of the 9th ACM International Conference on Systems
314 for Energy-Efficient Buildings, Cities, and Transportation (BuildSys '22)*, pages 1–10, 2022. doi:
315 10.1145/3563357.3564079.

- 316 Gautam Mandi, Fan Yang, Pushmeet Kohli, and Philip Torr. Decision-focused learning: Through the
317 lens of LP duality. In *ICML*, 2022.
- 318 Jay Mandi, Luca Furieri, Ferdinando Fioretto, et al. Decision-focused learning: Foundations, state
319 of the art, benchmark and future opportunities. *Journal of Artificial Intelligence Research*, 80:
320 1623–1701, 2024.
- 321 Lukas Schmidhuber and Dogan Keles. Carbon intensity nowcasting and forecasting for power grids.
322 *Applied Energy*, 2022.
- 323 Chris Thornton, Frank Hutter, Holger H. Hoos, and Kevin Leyton-Brown. Auto-WEKA: Combined
324 selection and hyperparameter optimization of classification algorithms. In *Proceedings of the 19th*
325 *ACM SIGKDD International Conference on Knowledge Discovery and Data Mining (KDD '13)*,
326 pages 847–855, 2013.
- 327 Bryan Wilder, Bistra Dilkina, and Milind Tambe. End-to-end learning and optimization: A survey. In
328 *IJCAI*, 2019.
- 329 Chen Xu, Kai Wang, and Yang Li. Carbonshift: Flexible load shifting for grid decarbonization. In
330 *ACM e-Energy*, 2023.
- 331 Wei Zhang and Jun Li. Smartci: Data-driven carbon intensity forecasting. *Energy Informatics*, 2020.